Soft-pulse dynamical decoupling in a cavity

Leonid P. Pryadko and Gregory Quiroz
Department of Physics & Astronomy, University of California, Riverside, California 92521, USA
(Received 31 August 2007; published 24 January 2008)

Dynamical decoupling is a coherent control technique where the intrinsic and extrinsic couplings of a quantum system are effectively averaged out by application of specially designed driving fields (refocusing pulse sequences). This entails pumping energy into the system, which can be especially dangerous when it has sharp spectral features like a cavity mode close to resonance. In this work we show that such an effect can be avoided with properly constructed refocusing sequences. To this end we construct the average Hamiltonian expansion for the system evolution operator associated with a single "soft" π pulse. To second order in the pulse duration, we characterize a symmetric pulse shape by three parameters, two of which can be made zero by shaping. We express the effective Hamiltonians for several pulse sequences in terms of these parameters and use the results to analyze the structure of error operators for a controlled Jaynes-Cummings Hamiltonian. When errors are cancelled to second order, numerical simulations show excellent qubit fidelity with strongly suppressed oscillator heating.

DOI: 10.1103/PhysRevA.77.012330 PACS number(s): 03.67.Pp, 03.67.Lx, 82.56.Jn

I. INTRODUCTION

Quantum coherent control has found its way into many applications, including nuclear magnetic resonance (NMR), quantum information processing (QIP), spintronics, atomic physics, etc. The simplest control technique is dynamical decoupling (DD), also known as refocusing. The goal of preserving coherence by averaging out the unwanted couplings is achieved most readily by running precisely designed sequences of uniformly-shaped pulses [1–3].

In a closed system, the corresponding performance can be analyzed in terms of the average Hamiltonian theory [4,5]. To leading order, the evolution over the refocusing period τ is indeed described by the time-averaged Hamiltonian of the system in the "rotating frame" defined by the control fields. Generally, the average Hamiltonian is constructed as a series in powers of τ. The number of the leading terms of this expansion that are exactly zero determines the order K of the refocusing sequence. Larger K implies asymptotically more accurate refocusing, with error terms scaling to zero faster with decreasing τ.

For an open system, the dynamics associated with the bath degrees of freedom can be also averaged out, as long as they are sufficiently slow. With leading-order ($K=1$) refocusing, the state decay processes are dramatically suppressed [6,7], with a moderate decrease of the dephasing rate [8], while with second-order refocusing ($K=2$) both decay and dephasing are strongly suppressed [8].

The decoherence analysis in Ref. [8] was based on the assumption of the low-frequency oscillator bath being near thermal equilibrium. This assumption becomes questionable if the bath has sharp spectral features—e.g., if the controlled qubit system is coupled to a local high-Q oscillator. On the other hand, such a situation where the controlled system is coupled to an oscillator mode is quite common. This situation is realized in atomic physics, where the oscillator in question is the cavity mode, while the continuous-wave (CW) excitation is used to suppress the coupling [9]. In several quantum computer designs, nearly linear oscillator modes are inherently present [e.g., mutual displacement in ion traps [10–14] or quantum computers (QCs) based on electrons on helium [15–18]]. Finally, there are suggestions to include local high-Q oscillators in the QC designs to serve as "quantum memory," [19] "quantum information bus," [20–22] or as a part of the measuring and control circuitry [23].

In this work we consider dynamical decoupling in a system where the spectral function of the oscillator bath has a sharp resonance. We include the resonant mode and the corresponding couplings in the system Hamiltonian and consider the dynamics of the closed system driven by the refocusing pulses applied to the qubits only. We construct the average Hamiltonian for a situation where one of the qubits is driven by a single symmetrical one-dimensional π pulse. To second order, the expansion is characterized by three parameters, two of which can be made zero by pulse shaping. An analysis of any refocusing sequence is then reduced to computing an ordered product of evolution operators for individual pulses. We illustrate the technique by analyzing the controlled dynamics of a single qubit coupled to an oscillator. One of the analyzed sequences provides an order $K=2$ qubit refocusing for any form of qubit–oscillator coupling. The simulations done for the Jaynes-Cummings Hamiltonian show excellent qubit fidelity with strongly suppressed oscillator heating, as long as the oscillator frequency bias exceeds the small coupling between the qubit and the oscillator remaining in the effective Hamiltonian. We argue that results of Ref. [8] for the corresponding open system remain applicable as long as this *renormalized* coupling is small compared to the resonance width.

II. BACKGROUND

A. Dynamical decoupling and effective Hamiltonian theory

The main idea of dynamical decoupling is to drive the system in such a way as to average out the effect of unwanted Hamiltonian couplings. Obviously, this only works if

the control fields are large compared with the other terms of the system Hamiltonian H_S.

The easiest situation to analyze is where "hard" δ-function pulses are used. In this case the system Hamiltonian can be ignored altogether during the action of the pulse. For a single qubit, a π pulse along the x axis corresponds to the evolution operator $X \equiv \exp(-i\pi s_x) = -i\sigma^x$, where $s_x = \sigma^x/2$ is the spin-1/2 operator. The evolution operator for a sequence of such pulses interrupting periods of free evolution can be written as a product of the corresponding unitaries. For example, the standard spin echo [24] sequence of a π pulse and a negative π pulse in the x direction followed by intervals of free evolution of equal duration τ corresponds to the operator

$$U_{X-\tau-\bar{X}-\tau-} = e^{-iH_S\tau}\bar{X}e^{-iH_S\tau}X. \tag{1}$$

Such expressions are easily simplified using the corresponding matrix algebra. For the case of NMR, the system Hamiltonian is that of the chemical shift,

$$H_S = \frac{1}{2}\Delta\sigma^z, \tag{2}$$

it anticommutes with the pulse unitary X, therefore $e^{-iH_S\tau}\bar{X} = \bar{X}e^{+iH_S\tau}$, and the two-pulse sequence (1) simplifies to the identity operator,

$$U_{X-\tau-\bar{X}-\tau-} = \bar{X}e^{+iH_S\tau}e^{-iH_S\tau}X = \bar{X}X = \mathbb{1}. \tag{3}$$

The simplicity of this formalism led to a number of strong mathematical results applicable to refocusing with ideal δ pulses. In particular, a succession of "concatenated" refocusing sequences provide an excellent refocusing accuracy which grows very rapidly with the number of pulses in a sequence [25,26].

In practice, however, the hard-pulse condition may be difficult to satisfy, and one has to account for the corrections associated with the action of the system Hamiltonian H_S during the pulse. If we denote the control Hamiltonian $H_C(t)$, the total Hamiltonian is

$$H(t) = H_C(t) + H_S. \tag{4}$$

The simplest first-order decomposition (e.g., see Ref. [3]) amounts to adjusting the intervals of free evolution before and after the pulse,

$$e^{-i(H_S+H_C)\tau} \approx e^{-iH_S\tau_1}e^{-iH_C\tau}e^{-iH_S\tau_2}, \tag{5}$$

where H_C is assumed time-independent, with the precise value of τ_1 and τ_2 computed in order to optimize the accuracy according to some fidelity measure. Superficially, any combination such that $\tau_1+\tau_2=\tau$ appears to provide equal accuracy to first order in τ. In fact, the accuracy of the expansion relies on both $H_S\tau$ and $H_C\tau$ being small; the results change non trivially for finite-angle rotations.

A more systematic way to analyze the effect of pulse shape is in terms of the average Hamiltonian theory [4,5]. This is equivalent to constructing the cumulant expansion of the evolution operator in powers of the system Hamiltonian in the interaction representation with respect to the control Hamiltonian $H_C(t)$ which is treated exactly.

For a system of qubits, the single-qubit control can be written most generally as

$$H_C(t) = \frac{1}{2}\sum_{n,\mu=(x,y,z)} V_n^\mu(t)\sigma_n^\mu, \tag{6}$$

where σ_n^μ, $\mu=x,y,z$ are the usual Pauli matrices for the nth qubit (spin). We assume that the qubit levels are nearly degenerate, or that Eq. (6) is written in the rotating wave approximation with respect to the qubit working frequency, so that the system Hamiltonian does not contain large terms. The control Hamiltonian [Eq. (6)] is a sum of single-qubit terms, and the zeroth order evolution operator which obeys the equation

$$\dot{U}_0(t) = -iH_C(t)U_0(t), \quad U_0(0) = \mathbb{1}, \tag{7}$$

can be constructed without much difficulty as a product of corresponding single-qubit operators. Then, the standard prescription is to separate the fast dynamics due to control fields out of the evolution operator by the decomposition $U(t) = U_0(t)R(t)$, and write the equation of slow evolution for $R(t)$,

$$\dot{R}(t) = -i\tilde{H}_S(t)R(t), \quad \tilde{H}_S(t) \equiv U_0^\dagger(t)H_S U_0(t). \tag{8}$$

The system Hamiltonian in the interaction representation, $\tilde{H}_S(t)$, is small at the scale of the refocusing period τ, which makes the time-dependent perturbation theory (TDPT) expansion applicable. The Magnus expansion, the exponentiated version of TDPT, has somewhat better convergence properties. It is written in terms of cumulants C_k,

$$R(t) = \exp[C_1(t) + C_2(t) + \cdots], \tag{9}$$

$$C_1(t) = -i\int_0^t dt_1 \tilde{H}_S(t_1), \tag{10}$$

$$C_2(t) = -\frac{1}{2}\int_0^t dt_2 \int_0^{t_2} dt_1 [\tilde{H}_S(t_1), \tilde{H}_S(t_2)], \quad \ldots. \tag{11}$$

Generally, the kth cumulant C_k contains a k-fold integration of the commutators of the rotating-frame Hamiltonian $\tilde{H}_S(t_i)$ at different time moments t_i and has an order $(tH_S)^k$.

Let us consider periodic dynamical decoupling with the period τ, $V_n^\mu(t+\tau) = V_n^\mu(t)$. In addition, we request that the zeroth order evolution operator (7) should also be periodic, $U_0(\tau) = \mathbb{1}$ (zeroth-order refocusing condition). Then, the Hamiltonian $\tilde{H}_S(t)$ is periodic, and the evolution operator over a time interval commensurate with τ, $\tau_n = n\tau$, can be factorized,

$$R(n\tau) = [R(\tau)]^n = \exp(-in\tau H_{ave}), \tag{12}$$

where the "average" Hamiltonian H_{ave} is defined in terms of cumulants,

$$-i\tau H_{\mathrm{ave}} = C_1(\tau) + C_2(\tau) + \cdots . \tag{13}$$

The main advantage of the average Hamiltonian theory is the improved convergence at large time: regardless of the value of t, the TDPT series needs to be convergent only at $|t| \leq \tau$.

B. Order of a refocusing sequence

For order-K refocusing, $K \geq 1$, we require additionally that the first K terms in the expansion of the effective Hamiltonian vanish, $C_1(\tau) = \cdots = C_K(\tau) = 0$. For a closed system, a refocusing sequence of higher order generally offers better scaling of accuracy with the sequence period. If we denote the maximum coupling in the system Hamiltonian as J (more precisely, $J = \|H_S\|$, a norm of the system Hamiltonian), the kth cumulant scales as $C_k \sim (J\tau)^k$, while the corresponding term in the average Hamiltonian $H_{\mathrm{ave}}^{(k)} \sim J^k \tau^{k-1}$. Consequently, for order-K dynamical decoupling, the refocusing error defined as the norm of the deviation of the unitary operator, $\delta_U = \|U(t) - \mathbb{1}\|$, scales as $\delta_U \sim (t/\tau)(J\tau)^{K+1}$, while the corresponding fidelity scales as $1 - F \sim \delta_U^2 \propto \tau^{2K}$. Thus, in the same system, a refocusing sequence of higher order can be run at a slower repetition rate.

Additional advantage of the effective Hamiltonian theory comes from its locality. The first-order effective Hamiltonian (cumulant C_1) contains only the qubit interactions present in the original Hamiltonian H_S. The cumulant C_2 contains connected pairs of such coupling terms. Generally, if we represent system Hamiltonian H_S as a graph, with qubits as vertices and two-qubit couplings as corresponding edges, the expansion of the kth order cumulant C_k can be represented as connected subgraphs with up to k edges. As a result, the first-order refocusing condition, $C_1(\tau) = 0$, can be verified by analyzing clusters with up to two qubits; second-order refocusing, with the additional condition $C_2(\tau) = 0$, requires analysis of all clusters with up to three qubits, etc.

This property, otherwise known as the cluster theorem [27], allows one to design *scalable* refocusing sequences whose refocusing order is independent of the system size. For a linear chain with nearest-neighbor interaction, one can achieve this by intermittently pulsing odd and even-numbered qubits. Several such particular sequences of order $K = 2$ and higher were demonstrated in Ref. [28].

C. Sequence order and open-system refocusing

Dynamical decoupling can be also effective against decoherence due to low-frequency environmental modes [29]. This can be understood by noticing that the driven evolution with period $\tau = 2\pi/\Omega$ shifts some of the system's spectral weight by the Floquet harmonics, $\omega \to \omega + n\Omega$. With the first-order average Hamiltonian for the closed system vanishing ($K = 1$ refocusing), the original spectral weight at $n = 0$ disappears altogether, and the direct transitions with the bath degrees of freedom are also suppressed as long as Ω exceeds the bath cutoff frequency, $\Omega \gtrsim \omega_c$ [6,7]. This corresponds to effective suppression of dissipative (T_1) processes.

The full analysis of decoherence, including both dissipative and reactive (T_2) processes, in the presence of order-K dynamical decoupling, $K \leq 2$, was done by one of the authors using the non-Markovian master equation in the rotating frame defined by the refocusing fields [8]. This involved a resummation of the series for the Laplace-transformed resolvent of the master equation near each Floquet harmonic, with subsequent summation of all harmonics.

The results of Ref. [8] can be summarized as follows. With $K \geq 1$ refocusing, there are no direct transitions, which allows an additional expansion in powers of the small adiabaticity parameter, ω_c/Ω. In this situation the decoherence is dominated by reactive processes (dephasing, or phase diffusion). With $K = 1$, the bath correlators are modulated at frequency Ω. This reduces the effective bath correlation time, and the phase diffusion rate is suppressed by a factor $\propto \omega_c/\Omega$. With $K = 2$ refocusing, all second-order terms involving correlators of the bath coupling at zero frequency, $\omega = 0$, are canceled. Generically, this leads to a suppression of the dephasing rate by an additional factor $\propto (\omega_c/\Omega)^2$, while in some cases (including single-qubit refocusing) all terms of the expansion in powers of the small adiabaticity parameter (ω_c/Ω) disappear. This causes an *exponential* suppression of the dephasing rate, so that an excellent refocusing accuracy can be achieved with relatively slow refocusing, $\Omega \gtrsim \omega_c$.

III. DYNAMICAL DECOUPLING OF A GENERICALLY-COUPLED QUBIT

The analysis in Ref. [8] was done for a generic thermal bath with a featureless quasicontinuous spectrum characterized by the upper cutoff frequency ω_c. The absence of sharp features justified an approximation where bath memory effects were essentially ignored at the scale of the decoherence time, although bath correlations at shorter times are crucial for describing the effects of dynamical decoupling. A sharp spectral feature, like a high-Q cavity mode, makes the starting point of the analysis [8], the non-Markovian master equation involving only qubits, questionable, unless the decoherence time *in the absence* of refocusing is long compared with the equilibration time of the high-Q mode.

A. Model

In this work we include any sharp quantum mode(s) into the "system" part of the Hamiltonian H_S, and consider the driven quantum dynamics of the resulting closed system. Compared with a system of qubits, a quantum oscillator admits a wider variety of linear or nonlinear couplings. By this reason we begin with a model of a qubit with most general couplings,

$$H_S = \sigma^x A_x + \sigma^y A_y + \sigma^z A_z + A_0, \tag{14}$$

where σ^μ are the qubit Pauli matrices and A_ν, $\nu = 0, x, y, z$ are the operators describing the degrees of freedom of the rest of the system which commute with σ^μ, $[\sigma^\mu, A_\nu] = 0$, but not necessarily with each other.

B. Pulse structure to linear order

First, consider the qubit evolution driven by a one-dimensional pulse,

$$H_C = \tfrac{1}{2}\sigma^x V_x(t), \quad 0 < t < \tau_p, \tag{15}$$

where the field $V_x(t)$ defines the pulse shape. The unitary evolution operator to zeroth order in H_S is simply

$$U_0(t) = e^{-i\sigma^x \phi(t)/2}, \quad \phi(t) \equiv \int_0^t dt' V_x(t'). \tag{16}$$

When acting on the spin operators, this is just a rotation, e.g., $U_0(t)\sigma^y U_0^\dagger(t) = \sigma^y \cos\phi(t) + \sigma^z \sin\phi(t)$.

For inversion pulses with the net rotation angle $\phi(\tau_p) = \pi$, with a symmetric shape, $V_x(\tau_p - t) = V_x(t)$, the average of the cosine over pulse duration is zero by symmetry,

$$\langle \cos\phi(t)\rangle_p \equiv \frac{1}{\tau_p}\int_0^{\tau_p} dt \cos\phi(t) = 0. \tag{17}$$

In such a case, the first two terms of the expansion, $X = X^{(0)} + \tau_p X^{(1)} + \tau_p^2 X^{(2)} + \cdots$, of the unitary evolution operator $X \equiv U(\tau_p)$ in powers of pulse duration τ_p read:

$$X^{(0)} = -i\sigma^x, \tag{18}$$

$$X^{(1)} = -A_x - \sigma_x A_0 + is(\sigma^y A_y + \sigma^z A_z). \tag{19}$$

Here the dimensionless parameter

$$s \equiv \langle \sin\phi(t)\rangle_p \tag{20}$$

is the only one that characterizes the pulse shape in this order.

We note that for π pulses the sine of evolution angle is nonzero only over the duration of the pulse; the time intervals before the beginning and after the end of the pulse where $V_x(t) = 0$ do not contribute to the value of s. Because of that, this parameter can be viewed as a measure of the effective duration of the pulse. For example, while $s = 0$ for an infinitely short δ pulse, for a Gaussian pulse [32] of width τ,

$$G_\tau(t + \tau_p/2) \equiv \frac{\pi^{1/2}}{\tau} e^{-t^2/\tau^2}, \quad \tau \ll \tau_p, \tag{21}$$

this parameter is $s \approx 1.5\tau/\tau_p$ (see Table I).

To create a pulse shape with effectively zero width to linear order, one can compensate for positive values of $\sin\phi(t)$ near the middle of the interval by making $V_x(t)$ somewhat negative near the beginning and the end of the interval. Such a first-order self-refocusing pulse was first suggested by Warren [30] as a "Hermitian" shape,

$$H_\tau(t + \tau_p/2) \equiv G_\tau(t + \tau_p/2)\frac{1 - \gamma t^2/\tau^2}{1 - \gamma/2}, \tag{22}$$

where the precisely computed value $\gamma = 0.960\,931\,721\,7$ is somewhat different from that in Ref. [30]. The corresponding fixed-length first-order self-refocusing pulse shapes S_L, with all derivatives up to and including the $(2L-1)$st vanishing at the ends of the interval, $L = 1, 2$, were constructed [28] in terms of their Fourier coefficients [31],

TABLE I. Parameters of several symmetric pulse shapes. The first line represents the "hard" δ-function pulse, $G_{0.05}$ denotes the Gaussian [32] pulse with the width $\tau = 0.05\tau_p$, see Eq. (21), $H_{0.05}$ is the corresponding Hermitian [30] pulse, see Eq. (22), while S_L and Q_L denote the first- and second-order self-refocusing pulses from Ref. [28], with up to $2L-1$st derivative vanishing at the ends of the interval of duration τ_p.

Pulse	s	$\alpha/2$	ζ
$\pi\delta(t-\tau_p/2)$	0	0	1/4
$G_{0.05}$	0.0744895	0.0349708	0.249476
$G_{0.10}$	0.148979	0.0653938	0.247905
$H_{0.05}$	0	0.00153849	0.249647
$H_{0.10}$	0	0.00615393	0.248589
S_1	0	0.0332661	0.238227
S_2	0	0.0250328	0.241377
Q_1	0	0	0.239889
Q_2	0	0	0.242205

$$V(t + \tau_p/2) = A_0 + \sum_m A_m \cos(m\Omega_p t), \tag{23}$$

where the angular frequency $\Omega_p = 2\pi/\tau_p$ is related to the full pulse duration τ_p; the coefficients A_m are listed in Ref. [28]. Compared to Hermitian pulse shape, the main advantage of pulses S_L is their smaller power [the maximum amplitude of the field $V(t)$].

For first-order self-refocusing pulse shapes such as H_τ or S_L, the terms proportional to s in Eq. (19) disappear, and the expansion of the unitary operator simplifies to

$$X_{s=0} = -i\sigma_x - \tau_p(A_x + \sigma_x A_0) + O(\tau_p^2). \tag{24}$$

C. Pulse structure to quadratic order

The structure of the pulse to quadratic order is easily computed as the next order in the TDPT. We have [cf. Eqs. (18) and (19)],

$$\begin{aligned} X^{(2)} = {} & + \frac{i}{2}[\{A_0, A_x\} + \sigma^x(A_0^2 + A_x^2)] + \zeta([A_0, \sigma^y A_z - \sigma^z A_y] \\ & + i\{A_x, \sigma^y A_y + \sigma^z A_z\}) + \frac{s}{2}(\{A_0, \sigma^y A_y + \sigma^z A_z\} \\ & - i[A_x, \sigma^y A_z - \sigma^z A_y]) + \alpha(A_y^2 + A_z^2 + i\sigma^x[A_y, A_z]) \\ & + \frac{s^2}{2}\{[A_z, A_y] + i\sigma^x(A_y^2 + A_z^2)\}, \end{aligned} \tag{25}$$

where we parametrized the pulse shape in terms of two additional parameters

$$\alpha \equiv \langle \theta(t - t')\sin[\phi(t) - \phi(t')]\rangle_p, \tag{26}$$

$$\zeta \equiv \langle \theta(t - t')\cos\phi(t')\rangle_p, \tag{27}$$

with the two-time averages over pulse duration

$$\langle f(t,t')\rangle_p \equiv \int_0^{\tau_p}\frac{dt}{\tau_p}\int_0^{\tau_p}\frac{dt'}{\tau_p}f(t,t'). \tag{28}$$

We also use the notations $[A,B]\equiv AB-BA$ for the commutator and $\{A,B\}=AB+AB$ for the anticommutator of two operators.

The effect of the parameter α was studied previously in Ref. [28]. The condition $\alpha=0$ is necessary to obtain NMR-style one-dimensional second-order self-refocusing pulses. Indeed, the corresponding system Hamiltonian is just that of the chemical shift, Eq. (2), thus $A_x=A_y=A_0=0$ and $A_z=\Delta/2$ in Eq. (14). Then, the evolution operator to quadratic order in $\bar{\tau}\equiv\tau_p\Delta/2$ is simply

$$X_\Delta = -i\sigma^x + is\bar{\tau}\sigma^z + \bar{\tau}^2(\alpha + i\sigma^x s^2/2) + O(\bar{\tau}^3), \tag{29}$$

the linear and quadratic corrections disappear entirely for second-order self-refocusing pulses such that $\alpha=s=0$. These are exactly the conditions used to design pulse shapes Q_L (Ref. [28]). The index $L=1,2$ denotes the parameter for the additional condition that the first $2L$ derivatives vanish at the ends of the interval, $V^{(l)}(0)=V^{(l)}(\tau_p)=0$, $l=0,\ldots,2L-1$.

The actual values of the parameters s, α, and ζ for several pulse shapes are listed in Table I. We note that for an ideal δ pulse, the parameters $s=\alpha=0$, whereas $\zeta=1/4$ is not particularly small. For all "soft" pulse shapes listed, the values of ζ are quite close to this value. The values of the parameter α are numerically small for all first-order self-refocusing pulses with $s=0$. The second-order self-refocusing pulses Q_1, Q_2 with $s=\alpha=0$ may work as a perfect replacement of δ pulses to second-order accuracy [28].

IV. COMMON PULSE SEQUENCES

Transforming Eqs. (19) and (25) appropriately, we can now easily compute the result of application of any pulse sequence. In particular, the π pulse $\bar{X}$ applied along the $-x$ direction can be obtained from $(-X)$ with the substitution $\alpha\rightarrow-\alpha$. As a result, e.g., the expansion of the evolution operator for the one-dimensional sequence $\bar{X}X$ [cf. Eq. (1)] can be written as

$$\bar{X}X = \mathbb{1} - 2i\tau_p[A_0 + \sigma^x A_x - s(\sigma^y A_z - \sigma^z A_y)] - 2\tau_p^2[A_0 + \sigma^x A_x - s(\sigma^y A_z - \sigma^z A_y)]^2 + O(\tau_p^3), \tag{30}$$

or it can be reexponentiated as evolution over time interval $2\tau_p$ with the average Hamiltonian

$$H_{\bar{X}X} = A_0 + \sigma^x A_x - s(\sigma^y A_z - \sigma^z A_y) + O(\tau_p^2). \tag{31}$$

We can attempt to correct for the terms proportional to s by using a longer sequence, e.g., $X\bar{X}\bar{X}X$. However, while the term is corrected in the leading-order effective Hamiltonian, we acquire a correction in the next order,

$$H_{X\bar{X}\bar{X}X} = A_0 + \sigma^x A_x - s\tau_p\{A_x, \sigma^y A_y + \sigma^z A_z\} + is\tau_p[A_0, \sigma^y A_z - \sigma^z A_y] + O(\tau_p^2). \tag{32}$$

While the external Hamiltonian A_0 cannot be averaged out by acting on the qubit, the term proportional to σ^x can be also suppressed with the help of two-dimensional sequences. The expression for the unitary $U_Y(\tau_p)\equiv Y$ resulting from application of the pulse along the y direction can be easily obtained from Eqs. (19) and (25) by cyclic permutation of indices. Then, for example, the refocusing sequence $\mathbf{4p}\equiv\mathbf{4p}(xy)\equiv X\bar{Y}XY$ corresponds to the effective Hamiltonian

$$H_{\mathbf{4p}} = A_0 + \frac{s}{2}(\sigma^x A_z - \sigma^z A_y) + \frac{i\tau_p}{2}[A_0, \sigma^x A_x - \sigma^y A_y] - \tau_p\frac{\alpha}{2}\sigma^y(A_x^2 + A_z^2) + \tau_p\frac{i\alpha}{2}[A_z, A_y] - \tau_p\frac{1+4\zeta}{4}\sigma^z\{A_x, A_y\} + O(\tau_p^2, s\tau_p), \tag{33}$$

where we dropped linear in τ_p terms proportional to s.

The symmetric 8-pulse sequence $\mathbf{8s}=YX\bar{Y}X\bar{X}\bar{Y}XY$ produces the effective Hamiltonian

$$H_{\mathbf{8s}} = A_0 + s\tau_p\left(\frac{i}{4}[A_z, A_x + A_y] + \frac{1}{2}(\sigma^x A_y^2 - \sigma^y A_x^2) + \frac{1}{4}\sigma^y\{A_x, A_y\} + \frac{1}{4}\sigma^z\{A_y, A_z\} + \frac{i}{2}\left[A_0, \sigma^y A_z + \sigma^z A_x + \frac{3}{2}\sigma^z A_y - \frac{5}{2}\sigma^x A_z\right]\right) - \frac{\alpha\tau_p}{2}\{\sigma^y(A_x^2 + A_z^2) + i[A_y, A_z]\} + O(\tau_p^2), \tag{34}$$

while the antisymmetric sequence $\mathbf{8a}\equiv\bar{Y}\bar{X}Y\bar{X}X\bar{Y}XY$ corresponds to

$$H_{\mathbf{8a}} = A_0 + \frac{s}{2}(\sigma^x A_z - \sigma^z A_y) + O(\tau_p^2). \tag{35}$$

We note that in the latter case there is a leading-order term proportional to s but no terms in order τ_p; this sequence produces second-order refocusing already with first-order pulses.

V. QUBIT IN A CAVITY

To illustrate these results, consider a qubit placed in a lossless cavity with a single mode nearly resonant with the qubit. We consider the simplest case where the system can be described by the Jaynes-Cummings Hamiltonian,

$$H_S = \omega_r b^\dagger b + \frac{\omega_0}{2}\sigma^z - g(b^\dagger\sigma_- + \sigma_+ b), \tag{36}$$

where $\sigma_\pm\equiv(\sigma^x\pm i\sigma^y)/2$, and ω_r and ω_0 are the frequency biases for the cavity and the qubit, respectively. Equation (36) can be also written in the form (14) with $A_x=-g(b+b^\dagger)/2$, $A_y=ig(b^\dagger-b)/2$, $A_z=\omega_0/2$, and $A_0=\omega_r b^\dagger b$. We concentrate on the special case $\omega_0=0$ which corresponds to working in the "rotating frame," with the control fields [Eq.

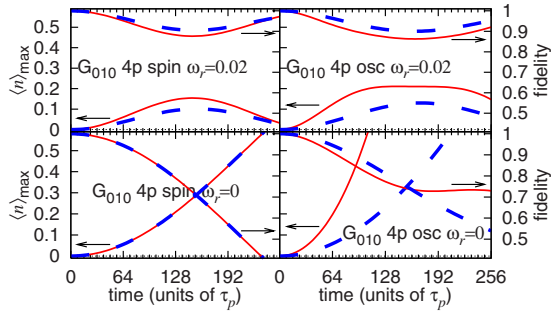

FIG. 1. (Color online) Evolution of the qubit fidelity and the number of quanta at the oscillator $\langle n\rangle$ (minimized and maximized over initial qubit states, respectively) at the end of the refocusing interval. Length-4 sequence **4p** with Gaussian pulses G_{010} applied on resonance with the qubit, $\omega_0=0$ in Eq. (36). Coupling constant $g=0.1/\tau_p$. Left panels: oscillator restricted to $n=0,1$ states, which makes it effectively a qubit. Right panels: oscillator restricted to $n\leq 8$ levels, which over the simulation time is equivalent to infinity. Bottom panels correspond to oscillator in resonance with the qubit, top panels correspond to oscillator frequency bias $\omega_r=0.02/\tau_p$. Solid lines correspond to control pulses applied along the x and y axes [sequence **4p**(xy)]; dashed lines correspond to control pulses applied along the x and z axes [sequence **4p**(xz)].

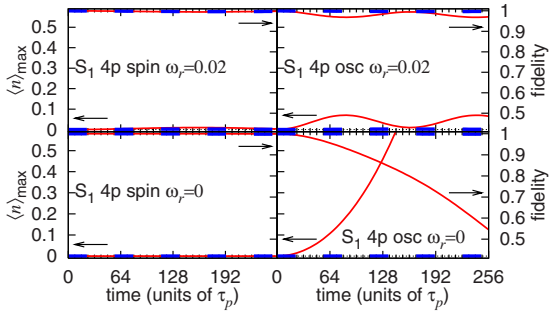

FIG. 2. (Color online) As in Fig. 1 but with first-order self-refocusing pulses S_1. The corresponding curves for pulses Q_1 (not shown) are virtually identical with linear scale.

(6)] applied on resonance with the qubit. Note that we assume the control fields to be applied directly at the qubit and not at the oscillator [23]; for a linear oscillator the corresponding compensation can be achieved by a spectral filter.

A. Sequence 4p

When the sequence **4p** is used with a Gaussian or other pulse shape with $s\neq 0$, the effective Hamiltonian to leading order can be written as

$$H_{\mathbf{4p}}=\omega_r b^\dagger b+\frac{s\omega_0}{4}\sigma^x-\frac{isg}{4}\sigma^z(b^\dagger-b)+O(\tau_p). \quad (37)$$

The original exchangelike oscillator coupling in Eq. (36) is replaced by the qubit phase coupling in Eq. (37). While the coupling magnitude is reduced by a small factor $\propto s$, it does not go down with more frequent pulse application. The same holds true if the oscillator is replaced by an auxiliary qubit (left panel in Fig. 1), or if the pulses are applied in the x-z direction [dashed lines in Fig. 1; the effective Hamiltonian is given by Eq. (39) below]. One can see from Fig. 1 that the refocusing accuracy is more or less similar for all these cases.

When the sequence **4p** is applied with first-order self-refocusing pulses (Hermitian or S_L), the first-order terms in the effective Hamiltonian are gone. This leaves terms linear in τ_p as the leading-order correction

$$H_{\mathbf{4p}}=\omega_r b^\dagger b-i\frac{\tau_p g\omega_r}{2}(\sigma_+ b^\dagger-\sigma_- b)-i\frac{1+4\zeta}{8}\tau_p g^2\sigma^z(b^2-\text{H.c.})+O(s,\alpha\tau_p,\tau_p^2), \quad (38)$$

where we set $s=0$ and dropped the relatively small term $\propto\alpha\tau_p$. We note that the first two terms in Eq. (38) disappear with $\omega_r=0$. The third term is suppressed when the oscillator is replaced by an auxiliary qubit ($b\to\tau_-$, $b^\dagger\to\tau_+$, $b^\dagger b\to\tau_z/2$). The same happens if the sequence is applied in the x-z direction [sequence **4p**$(xz)=X\bar{Z}XZ$], with the corresponding effective Hamiltonian

$$H_{\mathbf{4p}}^{(xz)}=\omega_r b^\dagger b+\frac{isg}{4}\sigma^x(b^\dagger-b)+\frac{s\omega_0}{4}\sigma^z-i\frac{\tau_p g\omega_r}{4}\sigma^x(b^\dagger-b)-\tau_p g\omega_0\frac{1+4\zeta}{8}\sigma^z(b^\dagger+b)+O(s\tau_p,\alpha\tau_p,\tau_p^2). \quad (39)$$

The net effect is that the refocusing accuracy is dramatically improved when the oscillator is replaced by an auxiliary qubit, or when the four-pulse sequence is applied on resonance ($\omega_0=0$) in the x-z plane using first-order pulses ($s=0$), with the oscillator also being in resonance with the qubit, $\omega_r=0$. In such cases, the only remaining linear in τ_p terms in the effective Hamiltonian are those proportional to the small parameter α, which allows for increased accuracy, see Fig. 2.

B. Sequence 8a

The antisymmetric eight-pulse sequence **8a** produces the effective Hamiltonian

$$H_{\mathbf{8a}}^{(xy)}=\omega_r b^\dagger b-\frac{isg}{4}\sigma^z(b^\dagger-b)+\frac{s\omega_0}{4}\sigma^z+O(\tau_p^2). \quad (40)$$

The refocusing is first-order with Gaussian pulses (Fig. 3), with the errors comparable to those of the sequence **4p** (cf. Fig. 1). The corresponding expression with pulses applied in the x-z plane [sequence **8a**(xz)] can be obtained by the substitution $\sigma^x\to\sigma^z$, $\sigma^z\to-\sigma^x$; this results in an almost identical performance (cf. dashed and solid lines in Figs. 3 and 4). With self-refocusing pulses S_1 [Fig. 4] or Q_1 (not shown) the sequence produces second-order refocusing. With all first- and second-order error terms canceled, the refocusing accuracy is improved dramatically.

C. Sequence 8s

The symmetric eight-pulse sequence **8s** produces the effective Hamiltonian

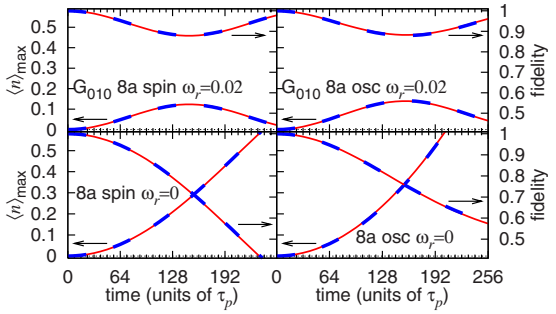

FIG. 3. (Color online) As in Fig. 1 but for the sequence **8a**. The term $\propto s$ in Eq. (40) produces large errors comparable for those for **4p** sequence in Fig. 1. This indicates that this sequence is less stable to pulse shape errors as compared to, e.g., the symmetric sequence **8s**.

$$H_{\mathbf{8s}}^{(xy)} = \omega_r b^\dagger b - \frac{\alpha\tau_p}{8}[g^2\sigma^y(b^\dagger + b)^2 - \omega_0^2\sigma^y] + O(\tau_p^2), \tag{41}$$

which corresponds to Eq. (38) with the larger terms already suppressed. The refocusing is first-order with either Gaussian (Fig. 5) or first-order pulses (see Fig. 6 with pulses S_1), and second-order with second-order pulses Q_L (not shown). With the linear scale of our plots, there is only a slight difference between zeroth and first order pulses (due to higher-order terms), and no visible difference between pulses S_1 and Q_1. When this sequence is applied in the x-z plane, we obtain

$$H_{\mathbf{8s}}^{(xz)} = \omega_r b^\dagger b - \frac{\alpha g^2\tau_p}{4}\sigma^y\{b^\dagger, b\} + O(\tau_p^2). \tag{42}$$

As can be also seen by comparing the dashed and solid lines in Figs. 5 and 6, the performance of this sequence depends little on how it is applied.

The performance of this sequence with self-refocusing pulses (e.g., S_1, Q_1) is also very close to that of the antisymmetric sequence **8a**. Nevertheless, the symmetric sequence **8s** provides better stability with respect to the pulse shape errors, and, according to results in Ref. [8], it is also expected to result in better visibility (smaller initial decoherence) when applied in an open system.

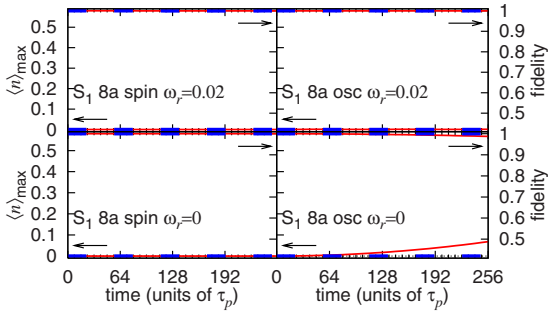

FIG. 4. (Color online) As in Fig. 1 but for the sequence **8a** with pulses S_1. The corresponding curves for pulses Q_1 (not shown) are virtually identical with linear scale.

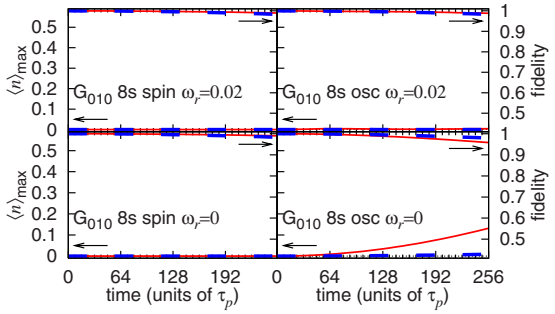

FIG. 5. (Color online) As in Fig. 1 but for the sequence **8s**.

D. Finite-width resonance

We analyzed in detail the performance of dynamical decoupling in a closed system. In particular, with properly designed refocusing fields, to an excellent accuracy, the quantum oscillator coupled to the qubit remains in the ground state, while the qubit fidelity remains very close to unity. Numerical results agree with the predictions from the analytically computed effective Hamiltonians which show greatly reduced coupling between the qubit and the oscillator. A very small frequency bias (of order of renormalized coupling value) becomes sufficient to effectively disconnect the oscillator mode and protect the qubit coherence.

A similar effect can be expected in an open system, where the resonant mode acquires a finite width Γ. For refocusing to be effective, Γ should exceed the renormalized qubit coupling. To test this prediction, we repeated the simulations with the imaginary oscillator frequency, $\omega_r = -i\Gamma$, while keeping all other simulation parameters the same as in Figs. 1–6. The corresponding results are shown in Fig. 7. While low-order sequences (e.g., 4-pulse sequence **4p** with Gaussian or S_1 pulses, bottom panes in Fig. 7, or sequence **8a** with Gaussian pulses) show rapid fidelity decay, the decay is substantially reduced for more accurate sequences. At the same

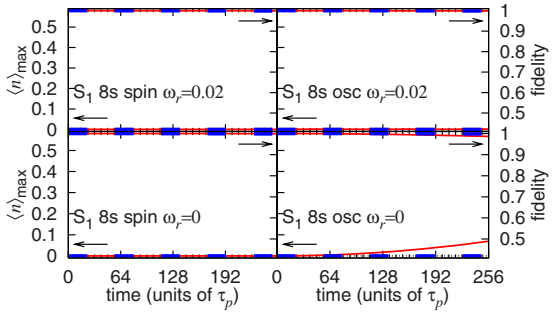

FIG. 6. (Color online) As in Fig. 1 but for the sequence **8s** with pulses S_1. Formally, the sequence is of the same order as with Gaussian pulses, see Fig. 5; the noticeable differences are due to error terms of higher order which we dropped in our calculations. The off-resonance refocusing is excellent (the fidelity and $\langle n\rangle$ curves in the top right panel run along the corresponding axes), while the on-resonance performance is also good. The plots with second-order pulses Q_1 (not shown) look almost identical. Note also that with the linear scale of these plots, the curves here are almost indistinguishable from those in Fig. 4.

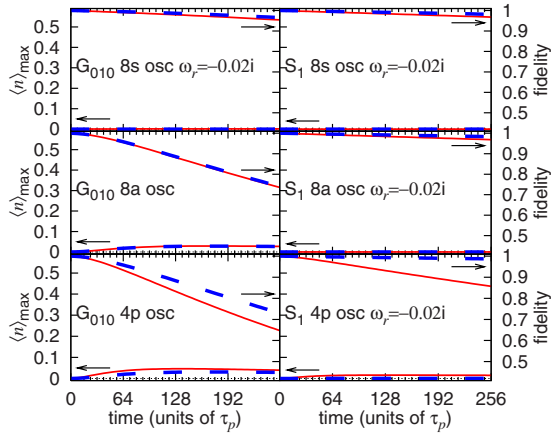

FIG. 7. (Color online) Refocusing with finite-width resonance at zero frequency bias. Simulation parameters as in Figs. 1–6 except that the oscillator frequency is taken to be purely imaginary, $\omega_r = -i\Gamma$. The curves show evolution of the qubit fidelity and the number of quanta at the oscillator $\langle n \rangle$ (minimized and maximized over initial qubit states, respectively) at the end of the refocusing interval. Left panes from bottom to top: sequences **4p**, **8a**, **8s** with Gaussian pulses G_{010} (cf. Figs. 1, 3, and 5, respectively). Right panes show the results of the simulation with pulses S_1 (cf. Figs. 2, 4, and 6, respectively). Oscillator is restricted to $n \leq 8$ levels, which over the simulation time is equivalent to infinity. Solid lines correspond to control pulses applied along the x and y axes [sequences **4p**(xy), **8a**(xy), **8s**(xy)]; dashed lines correspond to control pulses applied along the x and z axes [sequences **4p**(xz), etc.].

time, due to the decay, the number of quanta at the oscillator remains small.

We note that the simulation with $\omega_r = -i\Gamma$ corresponds to a (Markovian) thermal bath with very fast relaxation rate, which can be seen as the limit of very large upper cutoff frequency, $\omega_c \to \infty$. Strictly speaking, one does not expect the dynamical decoupling to be effective in this regime. The fidelity improvement in our simulations occurs because the spectral function of the Markovian environment is "filtered" through the resonant oscillator mode which results in a suppression of the high-frequency tail of the spectral function of the entire bath. While the effect is not as strong as we expect with true low-frequency bath (the upper cutoff frequency ω_c is small on the scale of the refocusing period Ω), there is a definite fidelity improvement.

To summarize, refocusing in the presence of a slow thermal bath characterized by the upper cutoff frequency can be effective even in the presence of sharp resonances in the spectral function. Specifically, this would happen as long as the renormalized qubit coupling with the resonant mode is small on the scale of the resonance width. This gives the modified, more broadly applicable, criterion for applicability of the results of Ref. [8]. In particular, we expect the second-order sequence **8s** with second-order pulses Q_n to provide an excellent refocusing accuracy to system Hamiltonian of Jaynes-Cummings form (36) also in the presence of a thermal bath, as long as the refocusing rate is sufficiently high. In addition to the condition on the renormalized value of the high-Q oscillator mode coupling, the refocusing period τ must be below the threshold value of order of the inverse bath cutoff frequency, ω_c^{-1}, see Ref. [8].

VI. CONCLUSIONS

In this work we analyzed the performance of soft-pulse dynamical decoupling in the presence of a sharp resonance mode. Because of the associated memory effects, such a problem cannot be addressed by considering master-equation dynamics for the qubit-system density matrix alone. Instead, we included the resonant mode and the corresponding couplings in the system Hamiltonian, and considered the dynamics of the resulting closed quantum system driven by a sequence of soft or hard refocusing pulses applied to the qubit. The analysis was done in terms of the effective Hamiltonian theory which describes the evolution of the system "stroboscobically" at the time moments commensurate with the refocusing period.

In fact, to make our results applicable to a large number of possible coupling terms between the qubit and the oscillator, we solved a more general problem of an arbitrary coupled [see Eq. (14)] controlled qubit. The main result of this work is the expansion of the unitary evolution operator Eqs. (19) and (25), and the classification of the corresponding parameters in Table I. This allows an explicit computation of the error operators associated with refocusing in systems of arbitrary complexity.

We also computed the effective Hamiltonians for several single-qubit refocusing sequences. To quadratic order, all coupling terms are canceled if the length-8 sequences **8a** [Eq. (35)] or **8s** [Eq. (34)] are used with first- or second-order self-refocusing pulses, respectively. We illustrated the general analytical results on the specific example of the driven Jaynes-Cummings Hamiltonian. The results of simulations agree with the predictions based on the analytically computed second-order effective Hamiltonians, although in some cases the effects of higher-order terms are noticeable.

For robust single-qubit refocusing, we recommend the symmetric 8-pulse sequence **8s**$=YX\bar{Y}XX\bar{Y}XY$ applied with second-order self-refocusing pulses. This sequence provides excellent refocusing accuracy for any form of the coupling of the qubit with the outside world, and it is stable with respect to pulse shape errors. As the second-order symmetric sequence, it should also work well for open systems, as long as the environment is slow on the scale of the refocusing rate [8]. The thermal bath is expected to remain close to equilibrium, and refocusing to perform well, as long as sharp features in the spectral function are wide on the scale of the *renormalized* value of the corresponding couplings.

ACKNOWLEDGMENTS

This research was supported in part by the NSF Grant No. 0622242 (L.P.) and the University of California, Riverside (G.Q.).

[1] C. P. Slichter, *Principles of Magnetic Resonance*, 3rd ed. (Springer-Verlag, New York, 1992).
[2] R. Freeman, Prog. Nucl. Magn. Reson. Spectrosc. **32**, 59 (1998).
[3] L. M. K. Vandersypen and I. L. Chuang, Rev. Mod. Phys. **76**, 1037 (2005).
[4] J. S. Waugh, L. M. Huber, and U. Haeberlen, Phys. Rev. Lett. **20**, 180 (1968).
[5] J. S. Waugh, C. H. Wang, L. M. Huber, and R. L. Vold, J. Chem. Phys. **48**, 662 (1968).
[6] A. G. Kofman and G. Kurizki, Phys. Rev. Lett. **87**, 270405 (2001).
[7] A. G. Kofman and G. Kurizki, Phys. Rev. Lett. **93**, 130406 (2004).
[8] L. P. Pryadko and P. Sengupta, Phys. Rev. B **73**, 085321 (2006).
[9] J. M. Villas-Boas, S. E. Ulloa, and N. Studart, Phys. Rev. B **70**, 041302 (2004).
[10] J. Cirac and P. Zoller, Phys. Rev. Lett. **74**, 4091 (1995).
[11] D. Vitali and P. Tombesi, Phys. Rev. A **59**, 4178 (1999).
[12] L. You, Phys. Rev. A **64**, 012302 (2001).
[13] D. Kielpinski, C. Monroe, and D. J. Wineland, Nature (London) **417**, 709 (2002).
[14] D. Vitali and P. Tombesi, Phys. Rev. A **65**, 012305 (2001).
[15] P. M. Platzman and M. I. Dykman, Science **284**, 1967 (1999).
[16] M. I. Dykman and P. M. Platzman, Fortschr. Phys. **48**, 1095 (2000).
[17] M. J. Lea, P. G. Frayne, and Y. Mukharsky, Fortschr. Phys. **48**, 1109 (2000).
[18] M. I. Dykman, P. M. Platzman, and P. Seddighrad, Phys. Rev. B **67**, 155402 (2003).
[19] E. J. Pritchett and M. R. Geller, Phys. Rev. A **72**, 010301 (2005).
[20] K. T. Kapale, G. S. Agarwal, and M. O. Scully, Phys. Rev. A **72**, 052304 (2005).
[21] L. F. Wei, Y. Xi Liu, and F. Nori, Phys. Rev. B **71**, 134506 (2005).
[22] M. R. Geller and A. N. Cleland, Phys. Rev. A **71**, 032311 (2005).
[23] A. Blais, J. Gambetta, A. Wallraff, D. I. Schuster, S. M. Girvin, M. H. Devoret, and R. J. Schoelkopf, Phys. Rev. A **75**, 032329 (2007).
[24] E. L. Hahn, Phys. Rev. **80**, 580 (1950).
[25] K. Khodjasteh and D. A. Lidar, Phys. Rev. Lett. **95**, 180501 (2005).
[26] K. Khodjasteh and D. A. Lidar, Phys. Rev. A **75**, 062310 (2007).
[27] *Phase Transitions and Critical Phenomena*, edited by C. Domb and M. S. Green (Academic, London, 1974), Vol. 3.
[28] P. Sengupta and L. P. Pryadko, Phys. Rev. Lett. **95**, 037202 (2005).
[29] L. Viola and S. Lloyd, Phys. Rev. A **58**, 2733 (1998).
[30] W. S. Warren, J. Chem. Phys. **81**, 5437 (1984).
[31] H. Geen and R. Freeman, J. Magn. Reson. **93**, 93 (1991).
[32] C. Bauer, R. Freeman, T. Frenkiel, J. Keeler, and A. J. Shaka, J. Magn. Reson. **58**, 442 (1984).